

Preparation of Tethered-Lipid Bilayers on Gold Surfaces for the Incorporation of Integral Membrane Proteins Synthesized by Cell-Free Expression

Angélique Coutable,^{†,‡,§,||} Christophe Thibault,^{||,⊥} Jérôme Chalmeau,[#] Jean Marie François,^{†,‡,§} Christophe Vieu,^{||,⊥} Vincent Noireaux,[#] and Emmanuelle Trévisiol^{*,†,‡,§,||}

[†]Université de Toulouse, INSA, UPS, INP, LISBP, 135 Avenue de Rangueil, F-31077 Toulouse, France

[‡]INRA, UMR792 Ingénierie des Systèmes Biologiques et des Procédés, F-31400 Toulouse, France

[§]CNRS, UMR5504, F-31400 Toulouse, France

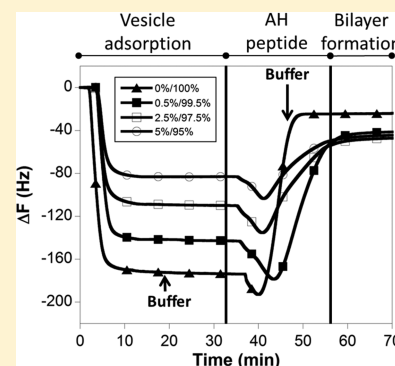
^{||}CNRS, LAAS, 7 avenue du Colonel Roche, F-31400 Toulouse, France

[⊥]Univ de Toulouse, INSA, LAAS, F-31400 Toulouse, France

[#]Physics Department, University of Minnesota, Minneapolis, Minnesota 55455, United States

Supporting Information

ABSTRACT: There is an increasing interest to express and study membrane proteins in vitro. New techniques to produce and insert functional membrane proteins into planar lipid bilayers have to be developed. In this work, we produce a tethered lipid bilayer membrane (tBLM) to provide sufficient space for the incorporation of the integral membrane protein (IMP) Aquaporin Z (AqpZ) between the tBLM and the surface of the sensor. We use a gold (Au)-coated sensor surface compatible with mechanical sensing using a quartz crystal microbalance with dissipation monitoring (QCM-D) or optical sensing using the surface plasmon resonance (SPR) method. tBLM is produced by vesicle fusion onto a thin gold film, using phospholipid-polyethylene glycol (PEG) as a spacer. Lipid vesicles are composed of 1-palmitoyl-2-oleoyl-*sn*-glycero-3-phosphocholine (POPC) and 1,2-distearoyl-*sn*-glycero-3-phosphoethanolamine-*N*-poly(ethyleneglycol)-2000-*N*-[3-(2-pyridyldithio)propionate], so-called DSPE-PEG-PDP, at different molar ratios (respectively, 99.5/0.5, 97.5/2.5, and 95/5 mol %), and tBLM formation is characterized using QCM-D, SPR, and atomic force technology (AFM). We demonstrate that tBLM can be produced on the gold surface after rupture of the vesicles using an α helical (AH) peptide, derived from hepatitis C virus NSSA protein, to assist the fusion process. A cell-free expression system producing the *E. coli* integral membrane protein Aquaporin Z (AqpZ) is directly incubated onto the tBLMs for expression and insertion of the IMP at the upper side of tBLMs. The incorporation of AqpZ into bilayers is monitored by QCM-D and compared to a control experiment (without plasmid in the cell-free expression system). We demonstrate that an IMP such as AqpZ, produced by a cell-free expression system without any protein purification, can be incorporated into an engineered tBLM preassembled at the surface of a gold-coated sensor.



1. INTRODUCTION

Biological membranes are constituted of a two-dimensional continuous lipid bilayer¹ containing a high density of proteins embedded within the bilayer or transiently attached to it.² They play a major role in information transfer and transport of ions and molecules between the inside and outside of the cell and mediate various intra- and extracellular processes.

The study of integral membrane proteins (IMPs) insertion into phospholipid bilayers, using techniques such as QCM-D and SPR, is essential for the development of new drug screening devices and for the investigation of various biological pathways. The insertion of IMPs at the surface of any biosensor requires first the formation of a mimetic lipid membrane. To incorporate integral membrane protein into preformed lipids bilayer, several approaches have been developed, mainly by the use of detergent.^{3,4} The detergent stabilizes and assists the

proper folding of the membrane protein by surrounding its hydrophobic core and allows its insertion within the lipid bilayer by destabilizing its structure. Supported lipid bilayers (SLBs), consisting of a bilayer assembly of phospholipids on a solid substrate,^{5–9} have been extensively used as model systems for development and applications in chemical biology,¹⁰ for biophysical studies and sensor design,^{11,12} and for cell biology.¹³ However, it has been reported that the close proximity of the SLB to the substrate limits the incorporation of transmembrane protein and causes their partial denaturation.¹⁴ Consequently, it is crucial to separate the lipid bilayer from the supporting solid substrate to minimize interactions of the protein with the substrate and to provide sufficient space

Received: June 28, 2013

for the correct conformation of transmembrane domains. Two kinds of planar lipid bilayer membranes can then be considered: (i) a tethered bilayer lipid membrane (tBLM), spaced from the surface by a tethering molecule (polymer cushion,^{15–17} peptide,¹⁸ protein¹⁹) or (ii) a lipid bilayer suspended on porous supports.¹¹ tBLM is often produced using lipids with thiol-,²⁰ disulfide-,²¹ and silane-²² modified headgroups, depending on the substrate, and are separated from the solid support by a hydrophilic spacer, which allows the creation of an hydrated reservoir between the surface of the solid support and the lipid bilayer.

One surface of choice for biosensing applications is gold, essentially due to its ease of functionalization via stable Au–thiolate bond formation and its electrical properties.^{23,24} However, it has been well-documented that due to the high polarizability of the gold surface, vesicles remain intact and stable on it^{5,25} without generating spontaneously any lipid bilayer. As a result, fabrication of tBLMs on gold requires additional preparation steps, mainly using a combination of Langmuir–Blodgett transfer and vesicle fusion²⁶ or gold modification¹⁶ prior to vesicle fusion. Recently, Wang and co-workers²¹ showed that tBLMs can be formed on unfunctionalized Au surfaces using phospholipid vesicles composed of 1-palmitoyl-2-oleoyl-*sn*-glycero-3-phosphocholine (POPC) and 1,2-distearoyl-*sn*-glycero-3-phosphoethanolamine-*N*-poly(ethyleneglycol)-2000-*N*-[3-(2-pyridyldithio)propionate] (DSPE-PEG-PDP) mixtures. The DSPE-PEG-PDP molecules are composed of a phospholipid moiety (DSPE), which will be inserted inside the lipid bilayer. PEG polymers act as spacer for lifting the lipid bilayer off the gold surface and thus provide a hydrophilic layer between the membrane and the gold surface (whose depth is around 4 nm when the bilayers are supported on a 3400 Da PEG cushion²⁷). The functional group PDP induces anchoring of the vesicles by forming Au–thiolate bonds at the gold surface. Alternatively, an amphipathic α -helix (AH) peptide derived from the N-terminus of the hepatitis C virus NS5A protein²⁸ could also induce bilayer formation on gold surfaces.^{29–32} The AH peptide interaction with the adsorbed vesicles is necessary, in addition to the vesicle–vesicle and vesicle–substrate interactions, to induce vesicle rupture on a gold surface. The AH peptide binds to the vesicle surface, promotes vesicle swelling, and then desorbs, leading to the formation of a lipid bilayer.³³

In the present work, we combine the incorporation of DSPE-PEG-PDP into vesicles and the effect of AH peptide to promote tBLM formation on the gold-coated surface of a biosensor. Vesicles are composed of different molar ratios of POPC and DSPE-PEG-PDP, respectively, 99.5/0.5, 97.5/2.5, and 95/5 mol %. Each tBLM formation is characterized using a quartz crystal microbalance with dissipation (QCM-D) monitoring, surface plasmon resonance (SPR), and atomic force microscopy (AFM). We use a cell-free expression system to produce the protein of interest, *E. coli* integral membrane protein Aquaporin Z (AqpZ), and to monitor the concurrent protein expression-incorporation into preformed tBLMs. Cell-free protein synthesis is becoming an alternative to cell-based protein expression, as it can deliver large amounts of proteins after a few hours of incubation. Originally developed to study transcription and translation processes, cell-free systems are now used in many studies ranging from basic research to large-scale experiments.³⁴ Different types of proteins including membrane proteins were successfully expressed by using cell-free expression systems.^{35–37} For example, the pore-forming

protein α -hemolysin was expressed inside large synthetic phospholipid vesicles to create a long-lived artificial cell system.³⁸ In the present study, the cell-free expression system producing the Aquaporin Z, an *E. coli* integral membrane protein, is directly incubated onto the tBLMs made of different lipid compositions. The incorporation of AqpZ is monitored by QCM-D and SPR, as it has been previously reported that these techniques allow the recording of membrane proteins insertion into a supported lipid bilayer.³⁹

2. MATERIALS AND METHODS

2.1. Materials. Phosphate buffer saline (PBS, 10 mM Na₂HPO₄, 137 mM NaCl, 2.7 mM KCl, pH 7.4) was purchased from Sigma. 1-Palmitoyl-2-oleoyl-*sn*-glycero-3-phosphocholine (POPC) and 1,2-distearoyl-*sn*-glycero-3-phosphoethanolamine-*N*-poly(ethyleneglycol)-2000-*N*-[3-(2-pyridyldithio)propionate] (DSPE-PEG-PDP) were obtained from Avanti Polar Lipids (Alabaster, AL). Amphipathic α -helical peptides (AH peptide) were purchased from Tebu-Bio (Le Perray-en-Yvelines, France).

2.2. Cell-Free Reaction. The crude extract was prepared with *Escherichia coli* BL21 Rosetta 2 cells according to Shin and Noireaux.^{40,41} The cell-free reaction was composed of 33% crude extract; the other 66% contained plasmids and the following components: 50 mM Hepes pH 7.6, 1.5 mM ATP and GTP each, 0.9 mM CTP and UTP each, 1 mM spermidine, 0.75 mM cAMP, 0.33 mM NAD, 0.26 mM CoenzymeA, 30 mM 3-phosphoglyceric acid (3-PGA), 0.068 mM folinic acid, 0.2 mg/mL tRNA, 1 mM IPTG, 1 mM each amino acid, 2% PEG 8000, 6.5 mM magnesium glutamate, 50 mM potassium glutamate. The endogenous *E. coli* RNA polymerase was used for expression.

2.3. Plasmid. The plasmids used in this study were constructed from the plasmid pBEST-Luc (Promega Corp., Madison, WI). *E. coli* sigma factor 28 was cloned under a Lambda promoter (plasmid pBEST-p15A-OR2-OR1-Pr-UTR1-Sigma28-T500,⁴¹ 0.5 nM final concentration).³⁹ The Aquaporin Z protein was cloned under a Ptar promoter specific to the *E. coli* sigma factor 28. The plasmid Ptar-AqpZ was used at a final concentration of 5 nM.

2.4. Vesicle Preparations. DSPE-PEG-PDP (molecular weight (MW): 2987.8 g/mol) and POPC (MW: 760.1 g/mol) phospholipids solutions dissolved in chloroform (10 mg/mL) were mixed in a 0.5/99.5, 2.5/97.5, and 5/95 molar ratio (mol %), respectively. The chloroform was removed under a stream of nitrogen, and subsequently evaporated for at least 3 h in a vacuum desiccator. Each phospholipid mixture film was resuspended in PBS buffer, to a final concentration of 2 mg/mL, and then vigorously stirred. Phospholipids vesicles were extruded (mini-extruder kit, Avanti Polar Lipid, Alabaster, AL) through polycarbonate membranes of 100, 50, and 30 nm pore size (31 times each). The size of each vesicle preparation was measured by dynamic light scattering (Malvern Zetasizer ZS, Malvern Instrument Ltd, UK), and the average diameter was 60 ± 2 , 62.1 ± 2.5 , and 59.5 ± 0.9 nm, respectively. Vesicles of different lipid compositions were then diluted in PBS buffer at a final concentration of 0.1 mg/mL.

2.5. Monitoring of Cell-Free Production by Quartz Crystal Microbalance with Dissipation. A Qsense E4 system and Qsoft software (Q-Sense, Sweden) were used for the QCM-D experiments. Gold-coated quartz crystals (QSX-301, Q-Sense, Sweden) were mounted in QCM-D flow chambers (QFM 401), in the Q-Sense E4 QCM-D sensor system.

Crystal sensors were cleaned by immersion in a freshly prepared solution of 5:1:1 H₂O/H₂O₂ (30%)/NH₄OH (25%) at room temperature for 5 min. They were extensively rinsed with ultrapure water and then dried under a nitrogen stream. Prior to being mounted in the flow chambers, the sensors were treated with oxygen plasma (200 W, 1.5 mbar, 5 min).

QCM-D chambers were first washed with PBS buffer at room temperature. The vesicle composition of interest (0.1 mg/mL, 1 mL per flow chamber) was injected simultaneously in both chambers at a flow rate of 100 μ L/min. After signal stabilization, flow chambers were rinsed with PBS buffer at 50 μ L/min during 20 min. AH peptide

solution (0.05 mg/mL, 1 mL per flow chamber) then was injected at a flow rate of 50 $\mu\text{L}/\text{min}$ to induce vesicle rupture, leading to bilayer formation on the gold surface of the crystals. Following bilayer formation on the surface of the sensor, QCM-D chambers were washed extensively with PBS buffer (50 $\mu\text{L}/\text{min}$, 20 min), and the temperature was brought to 30 °C. The baseline of Δf (frequency shift) and ΔD (dissipation variation) signals was reset to zero before injection of the cell-free extract (180 μL per flow chamber), 40 $\mu\text{L}/\text{min}$, then 20 $\mu\text{L}/\text{min}$ when cell-free reaction arrived in each flow chamber. The cell-free solutions were incubated for 3 h, without flow. The flow chambers were then rinsed with PBS buffer (20 $\mu\text{L}/\text{min}$, 20 min; 40 $\mu\text{L}/\text{min}$, 20 min; 80 $\mu\text{L}/\text{min}$, 20 min). The resonance frequency of the seventh overtone was chosen for data analysis, because it is less sensitive to crystal mounting conditions according to the manufacturer. The crystal sensor exhibited a fundamental resonance frequency of 5 MHz, giving a starting resonance frequency of 35 MHz for the seventh overtone.

2.6. Monitoring of Cell-Free Production by Surface Plasmon Resonance. A BiAcore 3000 biosensor (GE Healthcare) equipped with an Au sensor chip was used for surface plasmon resonance measurements. The Au sensor chip was cleaned as described for QCM-D sensors and mounted on the sensor chip support. The sensor chip was first washed with PBS buffer at 25 °C. Vesicle compositions of interest (100 μL , 10 $\mu\text{L}/\text{min}$) were injected in flow cells. Lipid surfaces were washed using PBS buffer (150 μL , 10 $\mu\text{L}/\text{min}$), and then AH peptide solution (100 μL , 0.05 mg/mL) was injected at a flow rate of 5 $\mu\text{L}/\text{min}$. Flow cells were finally rinsed with PBS buffer (200 μL , 5 $\mu\text{L}/\text{min}$). For optimizing cell-free expression, temperature was increased to 30 °C. After signal stabilization, 80 μL of cell-free expression system was injected at a flow rate of 5 $\mu\text{L}/\text{min}$, and the flow was stopped for 3 h. The flow cells were then washed with PBS buffer (100 μL , 5 $\mu\text{L}/\text{min}$).

2.7. Atomic Force Indentation Experiments. Force–distance curves were performed using a Nanowizard III (JPK Instrument, Berlin, Germany) at various steps of the tBLM formation process. Commercial AFM pyramid-shaped Si_3N_4 tips with an Au coating on the reflective side of the cantilever (MLCT-AUHW, Bruker) and a nominal spring constant of 0.01 N/m were used. Atomic force indentation experiments were performed at room temperature in PBS buffer. In these experiments, a constantly increasing force is applied by moving the tip toward the surface using the piezo-driven displacement at a rate of 1 $\mu\text{m}/\text{s}$. When an imposed maximal applied force is reached, the tip is automatically retracted. During these approaching/retracting cycles, the deflection of the cantilever, optically measured by the photodiode and translated after calibration into a force, is recorded. This treatment requires the precise knowledge of the spring constant of the cantilever, obtained by the thermal noise method,⁴² and the calibration of the force sensor, obtained by measuring the signal of the photodiode when the AFM tip is approached against a nondeformable hard substrate. For a surface covering of vesicles or lipid bilayers, plastic deformation events can be observed, which can be directly attributed to the punching of the vesicle or the bilayer. This punching gives a sharp jump of the cantilever tip, easily visible on the force/distance curve. The amplitude of this jump gives interesting information about the size of the plastically deformed structure. In this study, this method was used to distinguish between a layer of vesicles adsorbed on the surface and a tBLM. Intuitively, the jump for a lipid bilayer is comparable to the thickness of a bilayer (4–5 nm), while if a vesicle is under the tip, the jump will appear much larger and will depend on the vesicle size and its elasticity. To be quantitative, a large number of measurements (force/distance cycles) is required, and histograms plotting the amplitude of the observed jumps can be obtained. Finally, the method also relies on an adequate adjustment of the maximal applied force. This force needs to be larger than the breakthrough force, otherwise only plastic deformation of the vesicle or bilayer is observed, but not too excessive for not modifying irreversibly the surface under investigation. This latter concern is crucial when vesicles are present on the surface because, in this case, an excessive applied force during the first measurement is able to induce a long-range fusion of the vesicles, and the surface thus appears as a

bilayer for the rest of the measurements.⁴³ This is the reason two different maximal applied forces have been systematically investigated. A maximal force of 1.5 nN turned out to be appropriate for evidencing vesicle drilling, while, for lipid bilayers, higher maximal forces of 5 nN could be used to obtain a measurement of the bilayer thickness. Experimentally, a mica substrate (Jbg-Metafix, 24 × 32 mm) was freshly cleaved with adhesive tape just before gold deposition. Gold film of 100 nm was deposited by evaporation under vacuum (Evaporator Eva 600, Alcatel) at a 0.1 nm/s with a deposition temperature maintained at 150 °C.⁴⁴ Gold surfaces were cleaned in a solution of $\text{H}_2\text{O}:\text{H}_2\text{O}_2:\text{NH}_3$ (5:1:1), then rinsed with Milli-Q water and dried under a nitrogen stream. Just before experiments, these surfaces were rinsed with ethanol, Milli-Q water, and then dried under a stream of nitrogen. Vesicle compositions of interest were incubated 30 min, and then rinsed with PBS buffer. For surface measurement with AH peptide, the solution was incubated 1 h and then rinsed with PBS buffer. For all experiments, 1024 individual force–distance curves were collected in at least three different gold substrates and two different zones.

3. RESULTS

We investigated the experimental conditions to prepare tethered bilayer lipid membranes on gold-coated surfaces. The tBLMs were characterized by QCM, SPR, and AFM. The dynamic of the vesicle fusion process was monitored using the QCM. AFM force measurements, before and after the AH peptide incubation, demonstrated the crucial role of this peptide for the formation of a lipid bilayer. By comparing quantitatively QCM and SPR adsorption curves, we were able to evaluate the water content of the molecular assembly on the gold surface, which showed evidence of a tethering of the lipid bilayer induced by the PEG spacer. Finally, by using QCM-D and SPR measurements, we followed the incorporation of an integral membrane protein, AqpZ, after incubation of a cell-free expression system directly on the tBLMs.

3.1. tBLM Formation Process. To produce a tBLM, spaced from the supporting Au surface, we need to adjust the surface density of molecular spacers. In this work, the spacing is provided by the PEG chains added in controlled quantity to the vesicles, and the density of spacers is therefore adjusted by tuning the concentration of DSPE-PEG-PDP in the initial phospholipid mixture. To determine the best experimental conditions, we prepared different vesicles suspensions composed of DSPE-PEG-PDP and POPC mixtures (respectively, 0/100, 0.5/99.5, 2.5/97.5, and 5/95 mol %), and we monitored their adsorption on a gold surface by QCM-D, a technique pioneered by Kasemo's group to monitor supported lipid bilayer (SLB) formation.⁶ Each experiment was conducted four times for the four molar ratios investigated (Figure 1). The four different conditions, corresponding to the various concentrations of spacer molecule, behave quite similarly. Just after vesicle suspensions injection, a strong decrease of the resonance frequency indicates an adsorption of the vesicle at the surface of the gold sensor. After 5–10 min, the signal is stabilized, indicating that equilibrium is reached on the surface. At this step, vesicles are probably found on the surface, but it is not excluded that some of them spontaneously blew up. After AH peptide injection (0.05 mg/mL), the resonance frequency first decreases due to the fixation of the AH peptide to the vesicles, then starts to increase rapidly before reaching a stabilized value, showing again that at the end of the process, an equilibrium is reached at the sensor surface. This behavior can be explained by the role of the AH peptide, which induces a fusion of the vesicles.³² During this molecular reorganization, a large quantity of buffer solution, initially contained within or between the

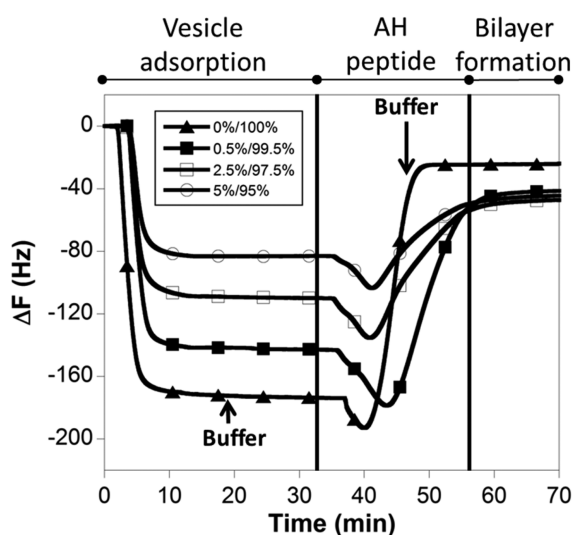


Figure 1. Quartz crystal microbalance (QCM) monitoring of three different tethered bilayer lipid membranes (tBLM) and one supported lipid bilayer (SLB) formation onto a gold-coated sensor. The curves show the shift of the mechanical resonance frequency (7th overtone) of the sensor with time after incubation of various vesicle mixtures. The respective vesicle compositions (0.1 mg/mL), \circ , 95 mol % POPC/5 mol % DSPE-PEG-PDP; \square , 97.5 mol % POPC/2.5 mol % DSPE-PEG-PDP; \blacksquare , 99.5 mol % POPC/0.5 mol % DSPE-PEG-PDP; \blacktriangle , 100% POPC, were injected leading to a resonance frequency decrease ($t = 0$ min, step 1). After buffer washing (indicated by an arrow), an AH peptide solution (0.05 mg/mL) was injected ($t = 35$ min, step 2). After buffer washing (indicated by an arrow), bilayers of different compositions are assembled on the sensor surface ($t = 55$ min, step 3).

vesicles, is released, inducing an increase of the resonance frequency. Three steps can then be distinguished in the QCM curves (Figure 1): (1) Vesicle adsorption before AH peptide injection, (2) AH peptide interaction and vesicle rupture, and (3) bilayer formation. The added mass at the end of step 1, as directly measured by the frequency shift after vesicle adsorption, depends on the content of DSPE-PEG-PDP. The higher is the content in DSPE-PEG-PDP, the less is the adsorbed mass at the end of step 1. This indicates that the modification of the phospholipid mixture impacts the density of vesicles adsorbed on the surface and the proportion of vesicles that spontaneously blow up. For the 5% molar ratio, at the end of step 1, the frequency shift is noticeably lower than for the other conditions, showing that, in this case, most of the vesicles spontaneously rupture before AH-peptide injection. At the end of step 3, after the bilayer formation at the Au surface, the

resonance frequency shifts of the three solutions containing 0.5%, 2.5%, or 5% of DSPE-PEG-PDP are not significantly different (Table 1). The final frequency shift averaged across the 0.5, 2.5, and 5 molar ratios of DSPE-PEG-PDP is around -45 Hz (four experiments). This value is significantly higher than the value expected for a supported lipid bilayer, which is known to be around -25 Hz.⁴⁵ This value is confirmed by our experiment conducted with the 100% POPC vesicles, which exhibited a final frequency shift of -23 Hz (Figure 1). This variation is tentatively interpreted by the difference of hydration of the molecules assembled at the surface. For pure POPC lipids, without any spacer, a supported lipid bilayer is produced (SLB) with a hydrated reservoir of around 1.7 nm²⁷ between the Au surface and the bilayer. When DSPE-PEG-PDP spacer molecules are mixed with the POPC phospholipids, QCM measurements reveal a higher added mass after bilayer formation, suggesting that water molecules are linked to the molecular assembly deposited at the sensor surface. This additional water content could be the signature of the tethering of the bilayer membrane (tBLM) including a liquid compartment between the bottom lipid layer and the Au substrate. However, we cannot exclude that some highly hydrated spacer molecules could also be assembled on the top of the lipid layer facing the solution. All together, QCM experiments show that, for the 0.5, 2.5, and 5 mol % of DSPE-PEG-PDP, a highly hydrated bilayer is formed on Au surface. The role of AH peptide is crucial for the low DSPE-PEG-PDP molar ratios likely because in this case vesicles do not spontaneously break on Au surface, but is less critical for high DSPE-PEG-PDP content for which vesicles spontaneously rupture.

To confirm the validity of the three steps observed during the QCM measurements, we performed AFM indentation experiments to distinguish the presence of vesicles at step 1 and the presence of a bilayer at step 3.

AFM measurements of force/distance curves have been performed on Au-coated mica surfaces supposed to be comparable with the QCM sensors presented in Figure 1. The final surface is mechanically tested after vesicle adsorption and buffer washing (after step 1 as referred to in Figure 1) or after AH peptide injection, bilayer formation, and buffer washing (after step 3 as referred to in the previous paragraph). All of the solutions with different spacer proportions have been considered, but for clarity and simplicity we only present the complete results obtained for a 99.5% POPC–0.5% DSPE-PEG-PDP molar ratio. Typical force/distance curves are shown before AH peptide incubation for a maximal applied force of 1.5 nN (Figure 2A) and after AH peptide action for a maximal applied force of 5 nN (Figure 2B). Most of the curves revealed

Table 1. Results from QCM-D and SPR (BIAcore) Measurements at the End of the Formation Process of a tBLM on a Gold-Coated Sensor (Four Different Experiments)^a

	QCM-D ($n = 4$)		BIAcore ($n = 4$)	
	ΔF (Hz)	mass (Voigt–Voinova model) (ng/cm ²)	response (RU)	mass (ng/cm ²)
95% POPC/5% DSPE-PEG(2000)-PDP	-49.1 ± 5.3	1464 ± 514	1693 ± 180	156 ± 17
97.5% POPC/2.5% DSPE-PEG(2000)-PDP	-47.1 ± 4.6	1798 ± 248	2143 ± 161	197 ± 15
99.5% POPC/0.5% DSPE-PEG(2000)-PDP	-36.1 ± 6.9	765 ± 154	1656 ± 362	152 ± 33

^aFrequency shifts as measured from the QCM-D were combined with the dissipation signal (not shown) for obtaining a “surface acoustic mass density” added at the sensor surface using the Voigt–Voivona model,⁴⁶ and variations of surface reflectivity measured in RU from the SPR system were converted in an “surface optical mass density” using a simple proportionality factor. The differences observed after mass density conversion between the two methods highlight the high hydration of the bilayer membrane formed at the gold-coated sensor surface attesting for a possible tethering of the bilayer by the PEG spacers.

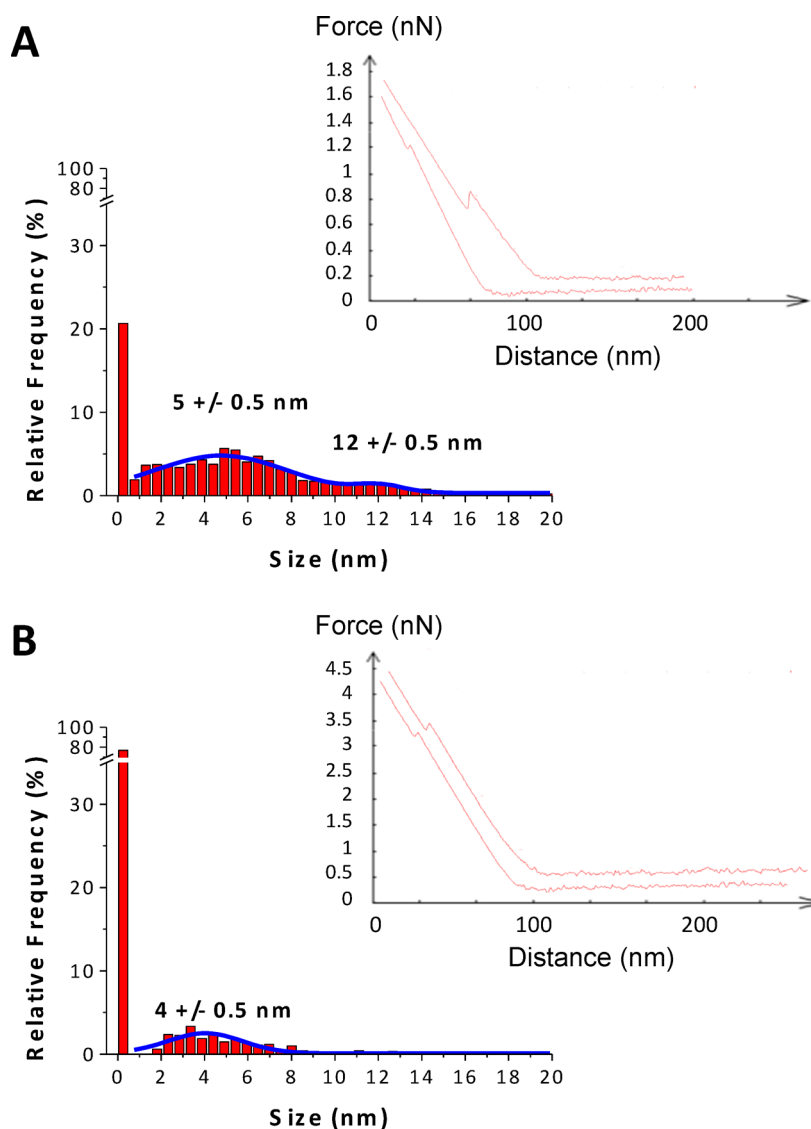


Figure 2. Rupture distance histograms ($n = 1024$ curves) and typical force/distance curves obtained by atomic force microscopy (liquid environment) on a gold-coated mica substrate incubated with a 99.5% POPC/0.5% DSPE-PEG-PDP vesicle mixture. (A) Before AH peptide incubation, with a maximal applied force of 1.5 nN. (B) After AH peptide incubation and buffer washing, with a maximal applied force of 5 nN.

the presence of abrupt jumps indicating the plastic indentation of the surface.

At step 1 (before AH injection, Figure 2A), we observe two groups of jumps. The first one occurred at a typical applied force around 0.7 nN and exhibited rupture distance centered around 12 nm. The second one occurred at a typical applied force of 1.2 nN and exhibited shorter rupture distance centered around 5 nm. A histogram of the rupture distance obtained after 1024 force/distance acquisitions is shown in Figure 2A. Events plotted at 0 correspond to the measurements with no sign of plastic indentation. Their proportion does not exceed 20%. The observation of two groups of plastic indentation events, with large rupture distances at low applied forces (1.2 nN) for one group, indicates that the surface is covered with unruptured vesicles. This result confirms our interpretation of the scenario of the bilayer formation elaborated after QCM measurement analysis, which starts at step 1 before AH peptide injection, by an adsorption of unruptured vesicles on the surface. As explained in the experimental section related to AFM experiments, if similar experiments were carried on using

higher maximal applied forces (5 nN), we observed a tip-induced fusion of these vesicles,⁴³ and the indentation curves (Supporting Information) revealed a lipid bilayer at the sample surface.

At step 3 (after AH injection and buffer washing, Figure 2B), we only observed one category of plastic indentation events. They occurred at an applied force around 3 nN and exhibited rupture distances centered around 4 nm. The histogram of rupture distances shows that, in this case, 80% of the measurements did not reveal any plastic indentation of the surface and that the average rupture distance is close to the nominal thickness of a bilayer. This result confirms that after step 3 the vesicles were ruptured due to the action of the AH peptide at step 2, resulting in a lipid bilayer formation at the sample surface. The same measurements performed at a lower maximal applied force of 1.5 nN never revealed rupture distances greater than 4 nm (Supporting Information) attesting that, indeed, unruptured vesicles are not present at the sample surface at the end of the process.

Finally, the AFM mechanical measurements confirmed that, except for high DSPE-PEG-PDP contents (5%), before the injection of the AH peptide the surface is mainly covered with unruptured fragile vesicles, which, after AH peptide action, blow up producing a bilayer at the sample surface. This confirms that in our experiments, at low surface density of molecular spacers, the role of the AH peptide is essential for obtaining a lipid bilayer on the gold surface of the sensor.

To clarify the degree of water content inside the molecular assembly formed at the gold-coated surface, we monitored the bilayer formation using the surface plasmon resonance (SPR) technique. Indeed, this optical method only reveals refraction index changes occurring during molecular adsorption at the sensor surface but is not sensitive to water molecules exhibiting no refraction index contrast with the buffer medium.⁴⁶ Therefore, by comparing QCM measurements, giving the total added mass at the surface including water molecules, with SPR measurements, we expected to be able to evidence a spacing of the bilayer membrane when DSPE-PEG-PDP linker is included in the vesicle composition. Each SPR experiment was achieved twice on two different chips ($n = 2 \times 2$), for the three investigated molar ratios.

The same behavior as for the QCM measurements shown in Figure 1 is observed, except that in this case an increase of the signal is the signature of an adsorption event (Figure 3).

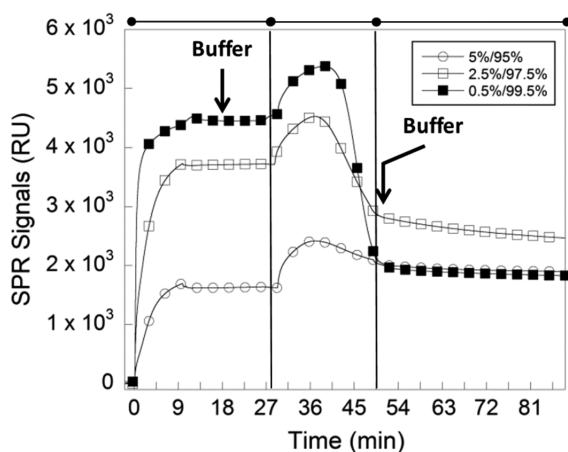


Figure 3. Surface plasmon resonance (SPR) measurements of three different tethered bilayer lipid membranes (tBLM) onto a gold-coated optical sensor. The curves show the variations of the surface reflectivity after incubation of various vesicle mixtures. The respective vesicle compositions (0.1 mg/mL), ○, 95 mol % POPC/5 mol % DSPE-PEG-PDP; □, 97.5 mol % POPC/2.5 mol % DSPE-PEG-PDP; ■, 99.5 mol % POPC/0.5 mol % DSPE-PEG-PDP, were injected leading to rapid adsorption of vesicles corresponding to an increase of the reflectivity ($t = 0$ min, step 1). After buffer washing (indicated by an arrow), an AH peptide solution (0.05 mg/mL) was injected ($t = 28$ min, step 2). After buffer washing (indicated by an arrow), bilayers of different compositions are assembled on the sensor surface ($t = 50$ min, step 3).

Following the same interpretation as given for the QCM curves (Figure 1), three steps can be distinguished in the SPR curves: (1) vesicle adsorption before AH peptide injection, (2) AH peptide interaction and vesicle rupture, and (3) lipid bilayer formation (Figure 3). The added material at the end of step 1, as directly measured by the increased surface reflectivity after vesicle adsorption, depends on the proportion of DSPE-PEG-PDP in the same manner as previously observed by QCM. This

effect indicates again that high DSPE-PEG-PDP content in the vesicle mixture increases the proportion of vesicles that spontaneously rupture on the Au surface after incubation. For larger DSPE-PEG-PDP contents, the effect of the AH peptide thus decreases because most of the adsorbed vesicles have spontaneously engaged a fusion process. However, at the end of step 3, after lipid bilayer formation at the Au surface, the final optical signals of the three solutions containing 0.5%, 2.5%, or 5% of DSPE-PEG-PDP are not significantly different on average when the experiment is carried out several times (Table 1).

Frequency shifts, as measured from the QCM-D, were combined with the dissipation signal (data not shown) for obtaining a “surface acoustic mass density” added at the sensor surface using the Voigt–Voivona model (Table 1).⁴⁷ The average value obtained at the end of step 3 over four experiments and three different vesicle composition is around 1340 ng/cm^2 . Variations of surface reflectivity, measured in RU from the SPR system, were also converted in a “surface optical mass density” using a simple proportionality factor ($1\text{RU} = 0.092 \pm 0.005 \text{ ng/cm}^2$).⁴⁸ The average value over four experiments and three different vesicle compositions is around 168 ng/cm^2 . The difference observed after mass density conversion between QCM and SPR is very significant. These rough estimations seem to indicate that approximately 80–90% of the added mass on the sensor surface corresponds to water molecules. This highlights the high hydration of the bilayer membrane formed at the gold-coated sensor surface attesting for a possible tethering of the bilayer by the PEG spacers.

3.2. Aquaporin Z Incorporation. In this section, the results obtained after production of the IMP AqpZ by a cell-free expression system directly incubated on tBLMs are presented. Through the monitoring of these experiments by QCM-D, we wanted to determine if the produced IMP proteins are able to interact with the tBLM preformed at the surface of the Au-coated sensor and eventually are inserted in the lipid bilayer. The interaction of cell-free expressed Aquaporin Z with the three tBLMs (0.5/99.5, 2.5/97.5, and 5/95 mol % of DSPE-PEG-PDP) was systematically characterized by QCM-D, but, for purposes of clarity, only the results obtained with 0.5% and 2.5% DSPE-PEG-PDP contents are presented. The cell-free expression system is a dense and viscous crude cell extract, which contains 10 mg/mL of proteins. Because the extract also contains the components required for coupled transcription-translation, such as tRNAs and ribosomes, that may interact nonspecifically with the tBLM, we systematically performed a control experiment in which the cell-free expression solution contains all of the components except the plasmid encoding for AqpZ. By comparing the results from the control fluidic chamber of the QCM-D system and those in which the AqpZ was expressed, we then could evaluate the interaction of the produced proteins with the tBLM quasi independently from the parasitic effects of the various constituents contained in the cell extract.

After tBLMs’ formation, according to the protocol described previously, a buffer washing is performed until stabilization of the QCM-D signals. The baseline of frequency shift Δf was then reset to zero before injection of the cell-free medium, and the temperature is raised to 30°C . As explained, the AqpZ-plasmid was added to the cell-free reaction mixture for the positive experiments but omitted for the control experiments. A volume of $180 \mu\text{L}$ of the final solution is then injected in each of QCM-D chamber. Changes in the seventh overtone resonant

frequency were recorded in real time over 4 h (Figure 4) from four curves: two for a tBLM produced with a DSPE-PEG-PDP molar ratio of 0.5 mol % and two for a tBLM composed of 2.5 mol % of DSPE-PEG-PDP.

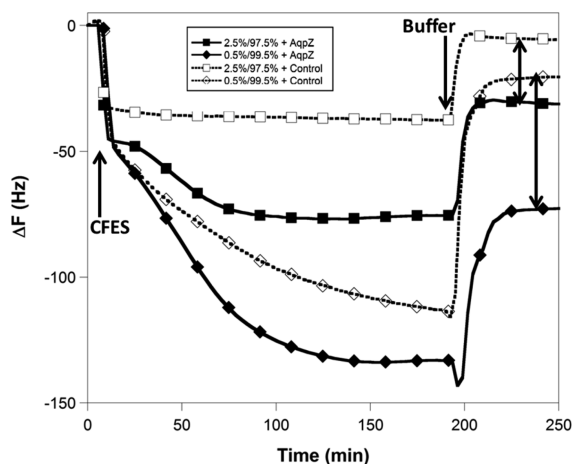


Figure 4. Quartz crystal microbalance measurements of Aquaporin Z produced by cell-free expression onto tBLMs (solid lines): ■, 97.5 mol % POPC/2.5 mol % DSPE-PEG-PDP; ◆, 99.5 mol % POPC/0.5 mol % DSPE-PEG-PDP. Dashed lines correspond to control experiments, that is, to cell-free expression without the addition of the AqpZ plasmid onto the 2 tBLMs: □, 97.5 mol % POPC/2.5 mol % DSPE-PEG-PDP; ◇, 99.5 mol % POPC/0.5 mol % DSPE-PEG-PDP. The cell-free solutions are injected at time 0 and left 3 h in the QCM chambers; washing with buffer solution is then performed. This final washing step removes a large quantity of material from the surface as observed by the brutal increase of the resonance frequency.

A resonance frequency shift of approximately -40 Hz was observed for all conditions, 10 min after the injection of the cell-free solution. It is known from previous studies that the beginning of AqpZ production starts after 20–30 min of incubation onto the tBLMs.³⁹ We assume that this resonance frequency shift is mainly due to the adsorption of various constituents of the cell-free expression system on the tBLM. Next, starting the description with a tBLM containing a lipid mixture of 97.5 mol % POPC/2.5 mol % DSPE-PEG-PDP, a clear difference between the control and the experiment where AqpZ is produced can be seen. For the later, at the onset of protein synthesis is observed a very large and progressive negative resonance frequency shift. This shift reaches -130 Hz after 3 h of expression. Conversely, for the control experiment without plasmid added in the cell-free expression system, during the same 3 h, the resonance frequency remains stable, attesting that no entity exhibiting specific affinity with the tBLM is produced inside the solution. After a final washing step, the curves of both the expression and the control experiments display an acute increase of the resonance frequency before final stabilization. This indicates that the washing step removes a large amount of molecular constituents only weakly attached to the tBLM. However, it is worth comparing the final resonance frequency of the control experiment ($\Delta f = -5$ Hz) after washing, which represents the amount of material coming from the cell-free expression system that binds tightly to the lipid bilayer, with the final resonance frequency of the experiment where AqpZ was produced ($\Delta f = -30$ Hz), which corresponds to the same amount of cell-free expression system components plus the

AqpZ proteins in interaction with the tBLM. This comparison clearly evidences that AqpZ proteins have been produced and were able to be incorporated inside the tBLM. The quantity of AqpZ in direct interaction with the tBLM after 3 h of cell-free expression on a tBLM containing a lipid mixture of 97.5 mol % POPC/2.5 mol % DSPE-PEG-PDP generates a resonance frequency shift of -25 Hz. A similar behavior was obtained for a tBLM containing a lipid mixture of 95 mol % POPC/5 mol % DSPE-PEG-PDP (data not shown). For a mixture of 99.5 mol % POPC/0.5 mol % DSPE-PEG-PDP, the final quantity of AqpZ found in the tBLM after the same duration of cell-free expression is even higher. In this case, the final resonance frequency of the control experiment is $\Delta f = -26$ Hz, while the final resonance frequency of the experiment where AqpZ was produced is $\Delta f = -81$ Hz. For this low content of DSPE-PEG-PDP molecules inside the tBLM, the shift in the resonance frequency due to the amount of AqpZ produced and attached to the tBLM after 3 h of cell-free reaction is as large as 55 Hz. To establish if the expressed protein AqpZ is incorporated inside the tBLM, we monitor the frequency and the dissipation signal in QCM-D. By plotting dissipation signal against the frequency signal ($D-f$ curve), we record the evolution of the softness or stiffness of the layer linked to the quartz sensor (Figure 5). For the control experiment, no significant change in

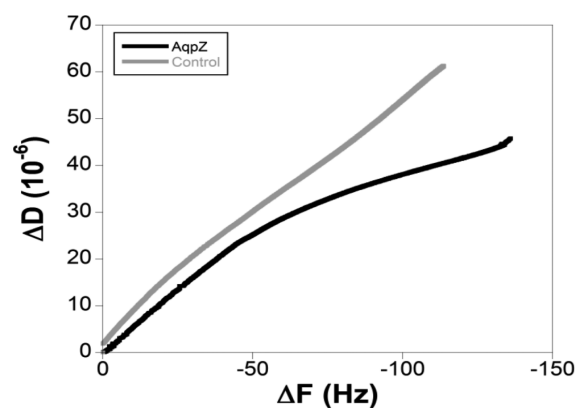


Figure 5. Dissipation against frequency ($D-f$) plots of cell-free expression of Aquaporin Z on 0.5% DSPE-PEG-PDP/99.5%POPC tBLM (black line) and control without addition of AqpZ plasmid (gray line).

the slope of the curve is observed. When AqpZ is produced by the cell-free reaction, the curve is drastically different from that obtained for the control. This could indicate that when the expressed AqpZ proteins are incorporated within the bilayer, the visco-elastic properties of the lipid membrane are modified in a way that decreases the amount of dissipation due to a stiffening of the layer. This trace thus seems to confirm the insertion of the proteins within the tBLM, but we cannot deduce from this experiment that the AqpZ is properly folded.

AqpZ insertion was also monitored through SPR experiments. The results for 2.5% and 0.5% of DSPE-PEG-PDP are shown in Figure 6. After cell-free injection, a sharp variation of reflectivity is observed, attesting that a large amount of adsorption events occurs on the lipid bilayer. When a plasmid encoding for AqpZ is present in the cell-free expression solution, the amount of material adsorbed on the bilayer increases progressively upon time, whereas for the control experiments the RU signal remains stable during 3 h. After buffer washing, indicated by an arrow in Figure 6, the signal

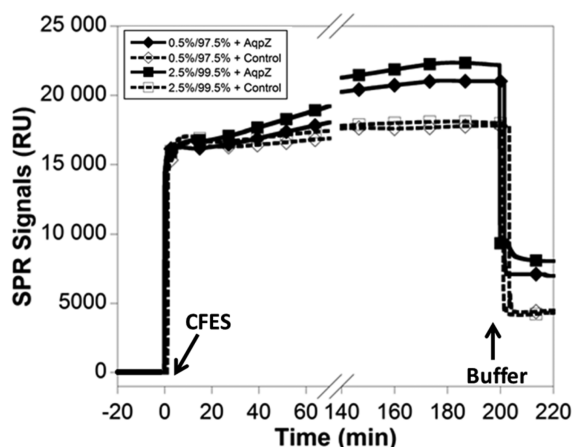


Figure 6. BIAcore measurements of Aquaporin Z produced by cell-free expression onto tBLMs (solid lines): ■, 97.5 mol % POPC/2.5 mol % DSPE-PEG-PDP; ◆, 99.5 mol % POPC/0.5 mol % DSPE-PEG-PDP. Dashed lines correspond to control experiments, that is, to cell-free expression without the addition of the AqpZ plasmid onto the 2 tBLMs: □, 97.5 mol % POPC/2.5 mol % DSPE-PEG-PDP; ◇, 99.5 mol % POPC/0.5 mol % DSPE-PEG-PDP. The cell-free solutions are injected at time 0 and left 3 h in the flow cells; washing with buffer solution is then performed. This final washing step removes a large quantity of material from the surface as observed by the brutal increase of the SPR signals.

drastically decreases, indicating that a large amount of the molecular material interacting with the lipid bilayer is removed. Very interestingly, after complete washing, a significant difference between the control experiments and the expression experiments is observed. On average of four assays, the control experiment indicates a RU signal of 3800, while for both DSPE-PEG-PDP contents, the signal after AqpZ expression raises 7000 RU. This difference may be attributed to the membrane proteins inserted inside the tBLM. All together, the SPR experiments confirm and complete QCM results and demonstrate that for both investigated molar ratios (2.5% and 0.5%), the insertion of AqpZ after cell-free expression is possible.

4. DISCUSSION

4.1. Fusion Process of Lipid Vesicles at Gold-Coated Surfaces. Vesicles fusion on gold surfaces usually requires chemical functionalization of the gold surface.^{49,50} However, by using phospholipid vesicles composed of DSPE-PEG-PDP and POPC mixtures, Wang et al. demonstrated that a tBLM could be produced directly on an unfunctionalized Au surface.²¹ When the disulfide of the PEG-lipopolymer DSPE-PEG-PDP binds to a gold surface, the sulfur–sulfur bond is cleaved in two separate thiolates entities,⁵¹ leading to the immobilization of DSPE-PEG-PDP via Au–thiolate bonds.¹⁶ Following this route, we also used DSPE-PEG-PDP and POPC mixtures in our experiments to generate a tethered BLM due to the PEG spacer attached to the DSPE lipids inserted in the bilayer. One result highlighted in our QCM-D and SPR measurements (Figures 1 and 3) is that the material adsorbed at the Au-coated surface after lipid injection strongly depends on the molar ratio of DSPE-PEG-PDP to POPC. We noticed that 5% DSPE-PEG-PDP results in a smaller adsorbed mass before AH peptide injection. One possible explanation for this observation is that the DSPE-PEG-PDP spacer increases the chemical affinity between vesicles and the gold surface that destabilizes the

vesicles.⁴³ Consequently, we can assume that under this condition, the high density of disulfide moieties leads to a spontaneous rupture of some vesicles²¹ and consequently to a release of water and to a smaller added mass. This is quite in good agreement with previous reports²¹ attesting that POPC/DSPE-PEG-PDP vesicles could spontaneously rupture on a gold surface without any additional procedure. However, in our experiments where the final objective is the incorporation of AqpZ inside this tBLM after cell-free expression, we cannot excessively increase the amount of DSPE-PEG-PDP molecules. Indeed, excess of DSPE-PEG-PDP may reduce the available space below the bilayer and moreover may possibly act as an antifouling agent when occasionally located on the top of the bilayer. This is the reason, in the present work, we investigated lower contents of DSPE-PEG-PDP spacer molecules. In that case, combined QCM, SPR, and AFM indentation experiments show that after the injection of the different vesicle mixtures, the fusion of the vesicles on the gold surface is not spontaneous and needs to be assisted. To induce the fusion of the vesicles on gold surfaces at low DSPE-PEG-PDP molar ratios, we used an amphipathic α -helix (AH) peptide derived from the N-terminus of the hepatitis C virus NSSA protein.²⁸ QCM-D and SPR measurements (Figures 1 and 3) clearly confirm the effect of this AH peptide, which, after fixation on the vesicles preadsorbed at the sensor surface, triggers their fusion resulting in the tBLM formation. The effect of this AH peptide is less relevant for the high concentration of DSPE-PEG-PDP spacer (5%) because, as explained previously, vesicles have already ruptured before AH-peptide injection. AFM indentation experiments (Figure 2) confirmed that before AH-peptide injection, vesicles can be found on the gold surface for a DSPE-PEG-PDP content of 0.5%, while after AH-peptide injection a lipid bilayer is formed on the surface.

4.2. Tethered Bilayer Lipid Membrane on Gold-Coated Surfaces. By comparing QCM and SPR data (Figures 1, 3 and Table 1), we could determine that 80–90% of the added mass as seen in QCM is related to water molecules. We interpret this added mass to the hydration of the PEG spacer layer embedded between the lipid bilayer and the Au surface due to the spacing PEG molecules randomly trapped inside the lipid bilayer. This high hydration rate was observed for all DSPE-PEG-PDP concentrations, indicating that the spacing effect does not require a huge proportion of DSPE-PEG-PDP spacer. The tethering of the bilayer membrane was also demonstrated by comparing the QCM final resonance frequency shift (Figure 1) when no DSPE-PEG-PDP spacer is involved (−23 Hz) with the final resonance frequency shift when this spacer is used (around −43 Hz). According to the Voigt–Voinova model,⁴⁷ this change in frequency shift gives a mass surface density of 405 ng/cm². If this difference is associated with water molecules, this translates into a water film thickness of around 4 nm. According to ellipsometric measurements,¹⁶ this thickness is in accordance with the thickness of pure DSPE-PEG-PDP films in water, which is comprised between 3.5 and 4 nm.¹⁶ All of these numerical estimations and experimental observations show that a tBLM is formed on a gold surface after the final fusion process involving the assistance of an AH peptide.

4.3. Aquaporin Z Incorporation into tBLMs. The results indicate that an IMP such as AqpZ can be produced by a cell-free expression system directly onto tBLMs preformed on a gold surface (Figures 4–6). The IMP interacts strongly with the lipid bilayer membrane, thus adding mass within the tBLM

and changing its mechanical properties by stiffening the layer (Figure 5). QCM-D and SPR measurements do not allow concluding that the IMP is correctly inserted and functional, but at least we have been able to optimize the structure of the tBLM for combining a spacing effect (by using a DSPE-PEG-PDP/POPC phospholipid mixture) with the assembly of the produced IMP AqpZ. We found that when a large proportion of PEG spacer is incorporated within the tBLM, the PEG chains occasionally located at the upper side of the lipid bilayer reduce the affinity of the produced IMPs with the lipid bilayer membrane, reducing their insertion. This work is an example of a technological compromise: DSPE-PEG-PDP molecules are necessary for detaching the lipid membrane from the Au-coated surface, a condition required for a correct incorporation of IMPs, but cannot be used in excess due to the antifouling properties of PEG spacers, hampering the insertion of the produced IMPs.

5. CONCLUSIONS

The perspective of producing membrane proteins and integrating them in a correct conformation at the surface of a sensor chip is a technological challenge of great interest for basic research and for many applications in biodetection or drug screening. This process is also a basic technological part when one is interested in fabricating hybrid systems combining silicon technology and biological nanomachines. Combining cell-free production of membrane proteins with the assembly of tethered lipid bilayers could be a possible route for achieving this purpose. In this Article, we have been interested in demonstrating this capability using a dedicated surface chemistry compatible with gold surfaces, which are often used in many sensing devices. Following previous proposals of the literature, we mixed POPC phospholipids with DSPE-PEG-PDP spacer to produce a tethered bilayer lipid membrane on gold surfaces. The separation of the bilayer from the gold surface is essential for incorporating integral membrane proteins. Indeed, dedicated experiments achieved by us before this work (data not shown) on conventional supported lipid bilayer (not tethered) were unsuccessful in demonstrating any insertion of IMPs. The combination of QCM, SPR, and AFM mechanical indentations experiments demonstrates the formation of a tethered lipid bilayer on gold surfaces and the effect of a viral amphipathic α -helix (AH) peptide for leading the fusion of the vesicles when the content of DSPE-PEG-PDP spacer is kept low. Cell-free production of AqpZ directly on these tBLMs results in an incorporation of the proteins. The present results do not demonstrate that the conformation of the integrated AqpZ inside the tBLM is correctly achieved. The next step of this study will be to demonstrate the functionality of inserted IMPs using this process.

■ ASSOCIATED CONTENT

● Supporting Information

Rupture distance histograms obtained by atomic force spectroscopy on a gold-coated mica surface incubated with DSPE-PEG-PDP/POPC vesicle mixture (0.5/99.5 mol %) before and after AH peptide action. This material is available free of charge via the Internet at <http://pubs.acs.org>.

■ AUTHOR INFORMATION

Corresponding Author

*E-mail: emmanuelle.trevisiol@laas.fr.

Notes

The authors declare no competing financial interest.

■ ACKNOWLEDGMENTS

This work was supported by the French National Research Agency (ANR) (FLANAMOVE project), by the University of Minnesota, and by the NSF grant PHY-075133. We thank Jonghyeon Shin for technical help. QCM-D experiments and AFM imaging were performed at the "Institut des Technologies Avancées en Sciences du Vivant" (Toulouse, France).

■ REFERENCES

- (1) Singer, S. J.; Nicolson, G. L. The fluid mosaic model of the structure of cell membranes. *Sciences (N.Y.)* **1972**, *175*, 720–731.
- (2) Spector, A. A.; Yorek, M. A. Membrane lipid composition and cellular function. *J. Lipid Res.* **1985**, *26*, 1015.
- (3) Picas, L.; Carretero-Genevri, A.; Montero, M. T.; Vazquez-Ibar, J. L.; Seantier, B.; Milhiet, P. E.; Hernandez-Borrell, J. Preferential insertion of lactose permease in phospholipid domains: AFM observations. *Biochim. Biophys. Acta* **2010**, *1798*, 1014–1019.
- (4) Berquand, A.; Levy, D.; Gubellini, F.; Le Grimellec, C.; Milhiet, P. E. Influence of calcium on direct incorporation of membrane proteins into in-plane lipid bilayer. *Ultramicroscopy* **2007**, *107*, 928–933.
- (5) Keller, C. A.; Glamästar, K.; Zhdanov, V. P.; Kasemo, B. Formation of supported membranes from vesicles. *Phys. Rev. Lett.* **2000**, *84*, 5443–5446.
- (6) Keller, C. A.; Kasemo, B. Surface specific kinetics of lipid vesicle adsorption measured with a quartz crystal microbalance. *Biophys. J.* **1998**, *75*, 1397–1402.
- (7) Lenz, P.; Ajo-Franklin, C. M.; Boxer, S. G. Patterned supported lipid bilayers and monolayers on poly(dimethylsiloxane). *Langmuir* **2004**, *20*, 11092–11099.
- (8) Richter, R. P.; Brisson, A. R. Following the formation of supported lipid bilayers on mica: A study combining AFM, QCM-D, and ellipsometry. *Biophys. J.* **2005**, *88*, 3422–3433.
- (9) Tamm, L. K.; McConnell, H. M. Supported phospholipid bilayers. *Biophys. J.* **1985**, *47*, 105–113.
- (10) Kiessling, V.; Domanska, M. K.; Murray, D.; Wan, C.; Tamm, L. K. Supported lipid bilayers: development and applications in chemical biology. *Wiley Encycl. Chem. Biol.* **2008**, *4*, 411–422.
- (11) Bally, M.; Bailey, K.; Sugihara, K.; Grieshaber, D.; Voros, J.; Stadler, B. Liposome and lipid bilayer arrays towards biosensing applications. *Small* **2010**, *6*, 2481–2497.
- (12) Castellana, E. T.; Cremer, P. S. Solid supported lipid bilayers: From biophysical studies to sensor design. *Surf. Sci. Rep.* **2006**, *61*, 429–444.
- (13) Yu, C. H.; Groves, J. T. Engineering supported membranes for cell biology. *Med. Biol. Eng. Comput.* **2010**, *48*, 955–963.
- (14) Tanaka, M.; Rossetti, F. F.; Kaufmann, S. Native supported membranes: creation of two-dimensional cell membranes on polymer supports (Review). *Biointerphases* **2008**, *3*, FA12.
- (15) Knoll, W.; Bender, K.; Forch, R.; Frank, C.; Gotz, H.; Heibel, C.; Jenkins, T.; Jonas, U.; Kibrom, A.; Kugler, R.; Naumann, C.; Naumann, R.; Reisinger, A.; Ruhe, J.; Schiller, S.; Sinner, E. K. Polymer-tethered bimolecular lipid membranes. *Adv. Polym. Sci.* **2010**, *224*, 87–111.
- (16) Munro, J. C.; Frank, C. W. Adsorption of lipid-functionalized poly(ethylene glycol) to gold surfaces as a cushion for polymer-supported lipid bilayers. *Langmuir* **2004**, *20*, 3339–3349.
- (17) Watkins, E. B.; El-khoury, R. J.; Miller, C. E.; Seaby, B. G.; Majewski, J.; Marques, C. M.; Kuhl, T. L. Structure and thermodynamics of lipid bilayers on polyethylene glycol cushions: fact and fiction of PEG cushioned membranes. *Langmuir* **2011**, *27*, 13618–13628.
- (18) Naumann, R.; Schmidt, E. K.; Jonczyk, A.; Fendler, K.; Kadenbach, B.; Leiebermann, T.; Offenhäusser, A.; Knoll, W. The peptide-tethered lipid membrane as a biomimetic system to

incorporate cytochrome c oxidase in a functionally active form. *Biosens. Bioelectron.* **1999**, *14*, 651–662.

(19) Giess, F.; Friedrich, M. G.; Heberle, J.; Naumann, R. L.; Knoll, W. The protein-tethered lipid bilayer: a novel mimic of the biological membrane. *Biophys. J.* **2004**, *87*, 3213–3220.

(20) Schiller, S. M.; Naumann, R.; Lovejoy, K.; Kunz, H.; Knoll, W. Archaea analogue thiolipids for tethered bilayer lipid membranes on ultrasmooth gold surfaces. *Angew. Chem., Int. Ed.* **2003**, *42*, 208–211.

(21) Wang, X.; Shindel, M. M.; Wang, S. W.; Ragan, R. A facile approach for assembling lipid bilayer membranes on template-stripped gold. *Langmuir* **2010**, *26*, 18239–18245.

(22) Atanasov, V.; Knorr, N.; Duran, R. S.; Ingebrandt, S.; Offenhausser, A.; Knoll, W.; Koper, I. Membrane on a chip: a functional tethered lipid bilayer membrane on silicon oxide surfaces. *Biophys. J.* **2005**, *89*, 1780–1788.

(23) Sackmann, E. Supported membranes: scientific and practical applications. *Science* **1996**, *271*, 43–48.

(24) Stelzle, M.; Weissmuller, G.; Sackmann, E. On the application of supported bilayers as receptive layers for biosensors with electrical detection. *J. Phys. Chem.* **1993**, *97*, 2974–2981.

(25) Reimhult, E.; Höök, F.; Kasemo, B. Intact vesicle adsorption and supported biomembrane formation from vesicles in solution: influence of surface chemistry, vesicle size, temperature, and osmotic pressure. *Langmuir* **2003**, *19*, 1681–1691.

(26) Shen, W. W.; Boxer, S. G.; Knoll, W.; Frank, C. Polymer-supported lipid bilayers on benzophenone-modified substrates. *Biomacromolecules* **2001**, *2*, 70–79.

(27) Kiessling, V.; Tamm, L. K. Measuring distances in supported bilayers by fluorescence interference-contrast microscopy: polymer supports and SNARE proteins. *Biophys. J.* **2003**, *84*, 408–418.

(28) Elazar, M.; Cheong, K. H.; Liu, P.; Greenberg, H. B.; Rice, C. M.; Glenn, J. S. Amphipathic helix-dependent localization of NSSA mediates Hepatitis C virus RNA replication. *J. Virol.* **2003**, *77*, 6055–6061.

(29) Cho, N. J.; Cho, S. J.; Cheong, K. H.; Glenn, J. S.; Frank, C. W. Employing an amphipathic viral peptide to create a lipid bilayer on Au and TiO₂. *J. Am. Chem. Soc.* **2007**, *129*, 10050–10051.

(30) Cho, N. J.; Cho, S. J.; Hardesty, J. O.; Glenn, J. S.; Frank, C. W. Creation of lipid partitions by deposition of amphipathic viral peptides. *Langmuir* **2007**, *23*, 10855–10863.

(31) Cho, N. J.; Frank, C. W.; Kasemo, B.; Hook, F. Quartz crystal microbalance with dissipation monitoring of supported lipid bilayers on various substrates. *Nat. Protoc.* **2010**, *5*, 1096–1106.

(32) Cho, N. J.; Wang, G.; Edvardsson, M.; Glenn, J. S.; Hook, F.; Frank, C. W. Alpha-helical peptide-induced vesicle rupture revealing new insight into the vesicle fusion process as monitored in situ by quartz crystal microbalance-dissipation and reflectometry. *Anal. Chem.* **2009**, *81*, 4752–4761.

(33) Cho, N. J.; Dvory-Sobol, H.; Xiong, A. M.; Cho, S. J.; Frank, C. W.; Glenn, J. S. Mechanism of an amphipathic alpha-helical peptide's antiviral activity involves size-dependent virus particle lysis. *ACS Chem. Biol.* **2009**, *4*, 1061–1067.

(34) He, M. Cell-free protein synthesis: applications in proteomics and biotechnology. *New Biotechnol.* **2008**, *25*, 126–132.

(35) Andreasson-Ochsner, M.; Fu, Z.; May, S.; Xiu, L. Y.; Nallani, M.; Sinner, E. K. Selective deposition and self-assembly of triblock copolymers into matrix arrays for membrane protein production. *Langmuir* **2012**, *28*, 2044–2048.

(36) Robelek, R.; Lemker, E. S.; Wiltschi, B.; Kirste, V.; Naumann, R.; Oesterheld, D.; Sinner, E. K. Incorporation of in vitro synthesized GPCR into a tethered artificial lipid membrane system. *Angew. Chem., Int. Ed.* **2007**, *46*, 605–608.

(37) Hovijitra, N. T.; Wu, J. J.; Peaker, B.; Swartz, J. R. Cell-free synthesis of functional aquaporin Z in synthetic liposomes. *Biotechnol. Bioeng.* **2009**, *104*, 40–49.

(38) Noireaux, V.; Libchaber, A. A vesicle bioreactor as a step toward an artificial cell assembly. *Proc. Natl. Acad. Sci. U.S.A.* **2004**, *101*, 17669–17674.

(39) Chalmeau, J.; Monina, N.; Shin, J.; Vieu, C.; Noireaux, V. alpha-Hemolysin pore formation into a supported phospholipid bilayer using cell-free expression. *Biochim. Biophys. Acta, Biomembr.* **2011**, *1808*, 271–278.

(40) Shin, J.; Noireaux, V. Efficient cell-free expression with the endogenous E. Coli RNA polymerase and sigma factor 70. *J. Biol. Eng.* **2010**, *4*, 8.

(41) Shin, J.; Noireaux, V. An E. coli cell-free expression toolbox: Application to synthetic gene circuits and artificial cells. *ACS Synth. Biol.* **2012**, *1*, 29–41.

(42) Butt, H. J.; Jaschke, M. Calculation of thermal noise in atomic-force microscopy. *Nanotechnology* **1995**, *6*, 1–7.

(43) Wang, X.; Shindel, M. M.; Wang, S. W.; Ragan, R. Elucidating driving forces for liposome rupture: external perturbations and chemical affinity. *Langmuir* **2012**, *28*, 7417–7427.

(44) Lebreton, C.; Wang, Z. Z. Nanofabrication on gold surface with scanning tunneling microscopy. *Microelectron. Eng.* **1996**, *30*, 391–394.

(45) Richter, R. P.; Lai Kee Him, J.; Brisson, A. Supported lipid membranes. *Mater. Today* **2003**, *6*, 32–37.

(46) Hook, F.; Stengel, G.; Dahlin, A. B.; Gunnarsson, A.; Jonsson, M. P.; Jonsson, P.; Reimhult, E.; Simonsson, L.; Svedhem, S. Supported lipid bilayers, tethered lipid vesicles, and vesicle fusion investigated using gravimetric, plasmonic, and microscopy techniques. *Biointerphases* **2008**, *3*, Fa108–Fa116.

(47) Voinova, M. V.; Rodahl, M.; Jonson, M.; Kasemo, B. Viscoelastic acoustic response of layered polymer films at fluid-solid interfaces: Continuum mechanics approach. *Phys. Scr.* **1999**, *59*, 391–396.

(48) Cooper, M. A.; Try, A. C.; Carroll, J.; Ellar, D. J.; Williams, D. H. Surface plasmon resonance analysis at a supported lipid monolayer. *Biochim. Biophys. Acta* **1998**, *1373*, 101–111.

(49) Ekeröth, J.; Konradsson, K.; Höök, F. Bivalent-ion-mediated vesicle adsorption and controlled supported phospholipid bilayer formation on molecular phosphate and sulfate layers on gold. *Langmuir* **2002**, *18*, 7923–7929.

(50) Wiegand, G.; Arribas-Layton, N.; Hillebrandt, H.; Sackmann, E.; Wagner, P. Electrical properties of supported bilayer membranes. *J. Phys. Chem. B* **2002**, *106*, 4245–4254.

(51) Ulman, A. Formation and structure of self-assembled monolayers. *Chem. Rev.* **1996**, *96*, 1533–1554.